RESEARCH ARTICLE / ARAŞTIRMA MAKALESİ

Synthesis, Characterization and Electrical Admittance Study of LaCrO₃Perovskite Compound

LaCrO₃ Perovskit Bileşiğinin Sentezi, Karakterizasyonu ve Elektriksel Admittans Çalışması

Mustafa COŞKUN[1] ⓘD

[1] *Istanbul Medeniyet University, Faculty of Engineering and Natural Sciences, Department of Engineering Physics, 34700 Uskudar, Istanbul, Turkey*

Abstract

We synthesized the ferroelectric perovskite oxide LaCrO₃ (LCO) using solid-state reaction method. Scanning electron microscope (SEM), energy x-ray dispersive (EDX) and X-ray diffraction (XRD) have been employed to study structural and chemical analysis of synthesized powder, respectively. Electrical admittance properties of the perovskite oxide sample was performed in wide range frequency (1Hz-10MHz) and temperature (-100 °C to +100 °C) using dielectric/impedance spectrometer. The results showed that the LCO has different activation energies and the calculated activation energies are of 0.175 eV and 0.220 eV from the G_{dc} *vs.* 1000/T and 0.152 eV and 0.197 eV from the f_{min} *vs.* 1000/T plots, respectively. The temperature-dependent exponent *s* showed that the overlapping large polaron tunneling (OLPT), quantum mechanical tunneling (QMT) and the correlated barrier hopping (CBH) conduction mechanism models can be suggested for the LCO compound.

Keywords: LaCrO₃, Perovskite Oxide, Admittance, Activation Energy,

Öz

Ferroelektrik perovskit oksit LaCrO₃'ü (LCO) katı hal reaksiyonu yöntemiyle sentezledik. Sentezlenen tozun yapısal ve kimyasal analizini yapmak için sırasıyla, taramalı elektron mikroskobu (SEM), enerji x-ışını dağılımı (EDX) ve X ışını kırınımı (XRD) yöntemleri kullanılmıştır. Perovskit oksit örneğinin elektriksel admittans özellikleri, dielektrik/empedans spektrometresi kullanılarak geniş bir frekans (1Hz-10MHz) ve sıcaklık (-100 °C ile +100 °C) aralığında gerçekleştirilmiştir. Sonuçlar, LCO' nun farklı aktivasyon enerjilerine sahip olduğunu ve hesaplanan aktivasyon enerjilerinin sırasıyla, G_{dc} & 1000/T grafiğinden 0.175 eV ve 0.220 eV, f_{min} & 1000/T grafiğinden de 0.152 eV ve 0.197 eV olduğu görülmüştür. Sıcaklığa bağlı s parametresi, örtüşen büyük polaron tünelleme (OLPT), kuantum mekaniksel tünelleme (QMT) ve ilişkili bariyer hoplama (CBH) iletim mekanizması modellerinin LCO bileşiği için önerilebileceğini göstermiştir.

Anahtar Kelimeler: LaCrO₃, Perovskit Oksit, Admittans, Aktivasyon Enerjisi.

I.INTRODUCTION

Perovskite-oxide materials stated by ABO₃ chemical formula, have considerable attention among the researchers due to their physical and chemical properties such as high crystallinity, high electrical conductivity, high stability in air, high temperature processability etc. Such unique properties of perovskite-oxides offer very large application areas including gas sensing [1], fuel cell [2], membrane [3], heating element [4], catalysis [5] so on. Researchers have synthesized and investigated many perovskite-oxide type compounds so far [6-9]. They proposed different routes such as solid-state reaction [10], Pechini method [11], hydrothermal reaction [12], microwave [13], sol gel [14], citrate gel combustion [15], etc. to synthesis perovskite-oxide compounds. Compare to the other synthesis methods solid-state reaction is still a favorable method employed by researchers due to the reduced the costs, less amount of chemical waste, minimizing side product and impurity formation, simple applying heat to the reaction and so on [16].

$LaCrO_3$ (LCO) is one of the important members of perovskite-oxide family with high optical band gap (3.4-3.5 eV), orthorhombic crystalline structure with a = 5.513 Å, b = 5.476 Å, c = 7.759 Å lattice parameters (space group P_{bnm}), high p-type conductivity, and high temperature durability in reducing atmosphere, high physical and chemical stability in air ambient etc. [17]. Although, researchers have investigated various properties of LCO compound, they mainly focused on the solid oxide fuel cell application [18-19]. So, the electrical properties of LCO still need to be investigated to understand its nature. K. Yoshii et. al [20] synthesized the LCO and studied its structural, chemical, dielectric and magnetic properties at room temperature. They reported the real and imaginary part of dielectric, conductivity and activation energy of the LCO at room temperature for two different frequency values (20 Hz and 1 kHz). S. M. Khetre et all [21] synthesized $LaCrO_3$ compound using solution combustion method and they studied its electrical and dielectric properties. They documented that the temperature dependent resistivity of LCO behaves like semiconductor. In addition, they studied frequency dependent dielectric constant of LCO at room temperature and it showed a dispersion based on electron-hole hopping mechanism, which is responsible for conduction and polarization. V. D. Nithya et al [22] synthesized $LaCrO_3$ and $LaCr_{0.5}M_{0.5}O_3$ (M= Cu and Fe) compounds using solution process method. They investigated their structural, chemical, electrical and magnetic properties. The results showed that undoped $LaCrO_3$ has 1.66×10^{-5} S/cm conductivity at room temperature and the doping Cu increased the conductivity while the doping Fe decreased the conductivity. As it can be seen from literature, there is no any comprehensive study in terms of wide temperature and frequency range on the electrical admittance properties, temperature dependent charge transport mechanism and activation energy of $LaCrO_3$ so there is a gap on the electrical and dielectric properties of $LaCrO_3$ compound.

In this study, beside the electrical admittance study structural and chemical nature of $LaCrO_3$ compound were studied. The powder compound was prepared via solid state reaction. Scanning electron microscopy (SEM), X-ray diffraction (XRD) and energy dispersive X-ray (EDX) analyses were employed to study surface characteristics, crystalline morphology and chemical nature of synthesized powder. A detailed study has been performed on the electrical admittance in wide range frequency (1 Hz to 10 MHz) and temperature (-100 °C to 100 °C) of LCO compound.

I. MATERIALS AND METHOD

Material synthesis and characterization have been reported in our previous work and details can be found in there [6]. The LCO powder was prepared by classic solid state reaction technique. In order to synthesis LCO powder, La_2O_3 (ACROS, 99.9%) and Cr_2O_3 (ACROS, 99%) powders were used as starting materials. First, the high purity La_2O_3 and Cr_2O_3 powders were mixed in an agate mortar for 1 h with ethanol and calcined at 900 °C for 10 h in the air to obtain LCO compound. After the first step calcination the powders were reground for homogeneity purpose. After reground the powder for several hours the second calcination was carried out at 1200 °C for another 12 h in the air. The chemical and structural analysis of LCO powder were carried out using a FEI scanning electron microscope (SEM), energy dispersive X-ray spectroscopy (EDX) and X-ray diffractometer (XRD, Bruker D8 Discover) analyses.

The LCO powder was pressed into 13 mm pellets at 10 tons pressure for several minutes in order to study electrical properties. After that, the pellet was heated at 1150 °C for 4 h in air to sinter the targets. Novocontrol Broadband Dielectric/Impedance Spectrometer was employed to study frequency-depended electrical admittance property measurements varied temperature from – 100 °C to 100 °C with 20 °C step. In order to investigate of electrical properties of LCO, the LCO pellet was sandwiched between two platinum (Pt) electrodes and placed into Dielectric Spectrometer for measurements.

II. RESULT AND DISCUSSION

SEM and EDX analyses of synthesized LCO are illustrated in Figure 1. As can be noticed from the Figures 1 (b) and (c) particles are not uniform and their sizes are variable. We can clearly see from the Figure 1 (c) particles have different sizes and the biggest one has over the 1 μm size. Figure 1 (d) displays the energy-dispersive X-ray (EDX) result of studied compound. The EDX analysis confirmed that our compound has La, Cr and O atoms with associated energies. The inset figures represents atomic ratio of elements inside the LCO. The XRD analysis of present compound was conducted and the result is shown in Figure 2. According to the XRD pattern the LCO compound has orthorhombic crystalline structure (PDF-01-070-2694 card) and all planes with associated two thetas are shown in Figure 2. Further XRD analysis results can be found in our previous study [17].
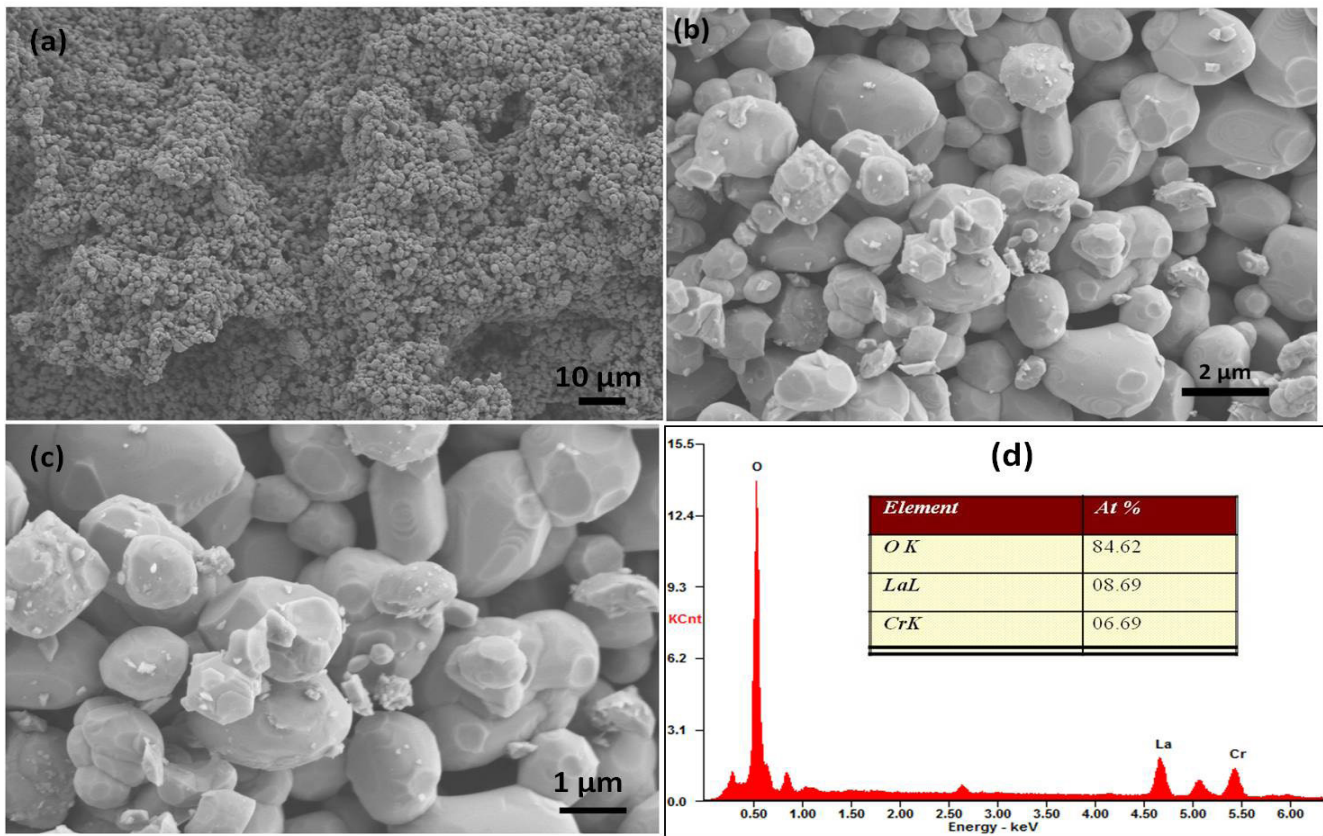
Figure 1. SEM micrographs of LCO (a) low, (b) middle and c) high magnification images, d) EDX analysis result of LCO.
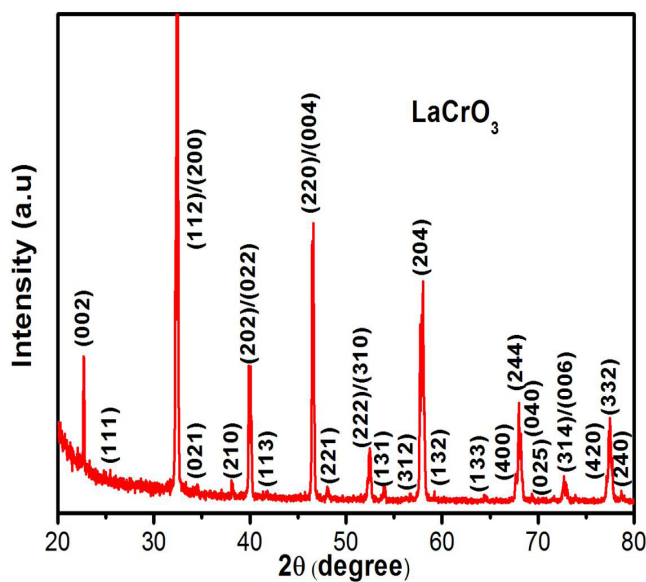

Figure 2. XRD pattern of LCO compound.

The complex admittance (Y^*) is an important parameter for dielectric materials and defined as follows [23]:

$$Y^* = \frac{1}{Z^*} = Y' + jY'' = G + jB \tag{1}$$

where Z^* is the complex impedance, Y' ($Re\ Y$) and Y'' ($Im\ Y$) real and imaginary ($Im\ Y$) parts of complex admittance and G is conductance and B is susceptance. The complex impedance, Z^*, can be written as [6]:

$$Z^* = R_s - jX \tag{2}$$

where R_s is series resistance or is called as capacitive reactance and X is called as inductive reactance. So, if we substitute equation (2) into the equation (1), the complex admittance, Y^*, can be rewritten as below:

$$Y^* = \frac{1}{R_s - jX} = Y' + jY'' = G + jB \tag{3}$$

$$\frac{1}{R_s - jX} = \frac{R_s + jX}{R_s^2 + X^2} = \frac{R_s}{R_s^2 + X^2} + j\frac{X}{R_s^2 + X^2} = Y' + jY'' = G + jB \tag{4}$$

$$Y' = \frac{R_s}{R_s^2 + X^2} = G \tag{5}$$

$$Y'' = \frac{X}{R_s^2 + X^2} = B \tag{6}$$

The real part of admittance (*Re Y*) or conductance (*G*) of the LCO is illustrated in Figure 3 (a). As can be seen from the figure the *G* has two different behavior depend on frequency. The first part is in the low frequency values that the *G* is frequency independent that called as dc region. It is clear that the *G* strongly depends on temperature and increases with increasing temperature. The dc region extends to the higher frequency with increasing temperature. The second part is in the high frequency and the *G* strongly depends on frequency values so this region is called as ac region. It is noticed that the ac region has two different linear slopes. These slopes are related charge transport phenomenon in the compounds and different slopes mean different charge transport mechanisms [6]. Figure 3 (b) shows frequency dependent the imaginary part of admittance (*Im Y*) or susceptance (*B*) of the LCO at various temperature.

The negative values indicate capacitive effect is dominant rather inductive effect. The *Im Y* decreases with increasing frequency then reaches a minimum value and start increases with increasing frequency between – 100 °C and 0 °C. However, this behavior is a little bit different between 0 °C and 100 °C. In this region, the *Im Y* first increases with frequency and reaches a maximum value, then decreases

with increasing frequency finally reaches a minimum value then increases with increasing frequency again. Those minimum and maximum values indicate the relaxation process in the studied compound. Furthermore, those maximum and minimum values shift through higher frequency with increasing temperature which indicate the relaxation process is highly thermally affected. Figure 3 (c) illustrates the *Re Y vs. – Im Y* plots (or Cole-Cole plot) of the LCO at various temperature. It is clear from the plots that there are two different regions: the first region is the low frequency region and the *Im Y* decreases sharply till a certain value (like a vertical line) or minimum value whereas the *Re Y* remain almost constant. After *Im Y* reaches a minimum value both *Im Y* and *Re Y* increase together which is the second region and this region relatively includes higher frequency region. Moreover, these minimum values both increase and shift through the right side with increasing temperature that indicate relaxation process is thermally activated [24].

We have calculated the activation energy of LCO compound via employing the temperature dependent relaxation frequency from the – *Im Y vs. logf* and the dc conductance region from *Re Y vs. logf* plots, which are given by Arrhenius relations [24]:
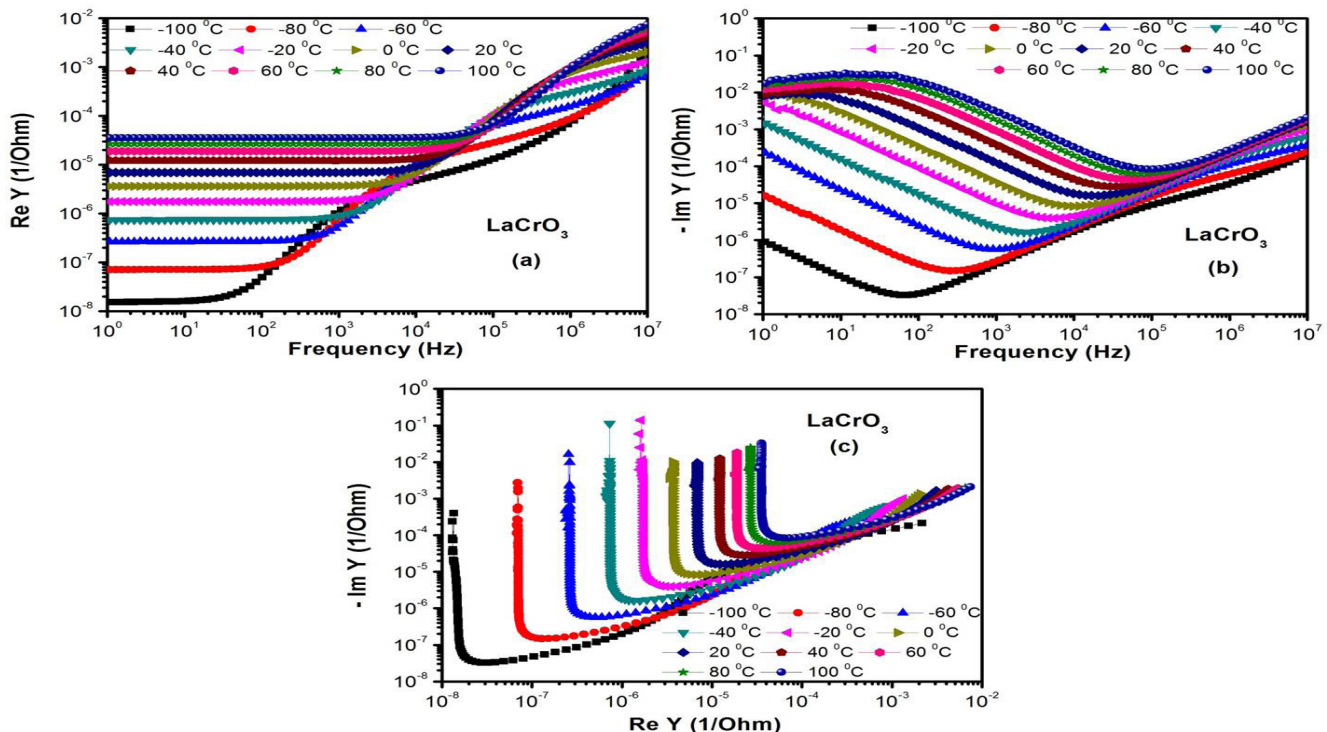

Figure 3. The real (a) and imaginary part (b) of admittance and (c) Re Y vs. – Im Y (c) plots of LCO.

$$f_{min} = f_0 \, e^{\left(-\frac{E_a}{k_B T}\right)} \quad (7)$$

$$G_{dc} = G_0 \, e^{\left(-\frac{E_a}{k_B T}\right)} \quad (8)$$

where f_{min}, f_0, G_{dc}, G_0, E_a, k_B and T are values at min. frequency in the $-$ *Im Y vs. logf* plots, a constant related to frequency, dc conductance from *Re Y vs. logf* plots, a pre-exponential factor for dc conductivity, activation energy, boltzman constant and temperature in Kelvin scale, respectively. The activation energy, E_a, extracted from the both G_{dc} *vs. 1000/T* and f_{min} *vs. 1000/T* plots. It can be noticed from the Figure 4 that the LCO compound has two different regions denoted as *Region I* and *Region II*. The calculated activation energy was denoted as E_{a1} for *Region I* and E_{a2} for *Region II*. In the *Region I*, the activation energy was calculated as 0,175 eV from the G_{dc} *vs. 1000/T* plot and f_{min} *vs. 1000/T* plot. The activation energy for *Region II* was calculated as 0,220 eV and 0,197 eV from the G_{dc} *vs. 1000/T* and f_{min} *vs. 1000/T* plots, respectively. As can be seen each activation energy pretty close each other for LCO. Such activation energy values have been obtained for
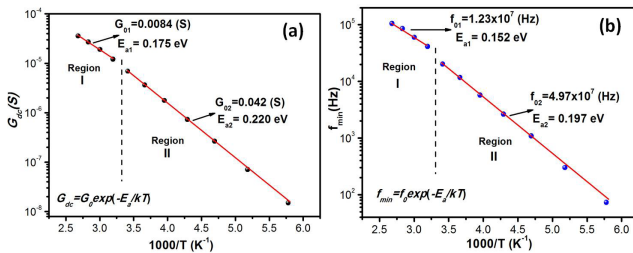

Figure 4. Semilog a) (G_{dc}) versus (1000/T), b) (f_{min}) versus (1000/T) plots for LCO.

many perovskite type compounds in literature before [6, 10, 24,]. Two different activation energy values for the LCO can be related different charge transport phenomena. In order to proof this different charge transport phenomena we plotted frequency depended absolute admittance $|Y|$ plots with different temperature ($|Y| = \sqrt{(Re\ Y)^2 + (Im\ Y)^2}$). Figure 5 (a) shows the *IYI vs. f* plots of LCO compound. It is clear that the frequency dependence behavior of the $|Y|$, is so similar to *Re Y*. The $|Y|$, has two different regions: the first one is low frequency region and as can be seen from the Figure 5 (a) this region called as dc region and is frequency independent. The second one is high frequency region which the $|Y|$ strongly depends on frequency and called as ac region.
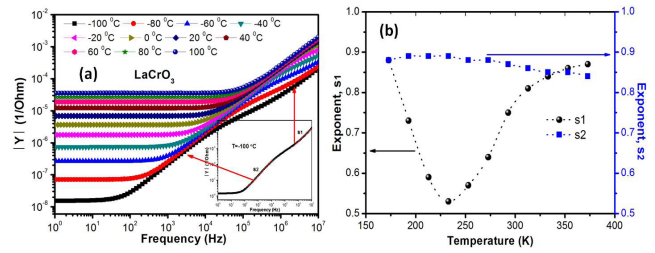

Figure 5. a) Frequency dependent the total admittance (or conductance) plot (inset figure show linear slopes in the ac region), b) Temperature dependent variation of exponent *s*.

Hence the conductance, G, or $|Y|$ consists two parts (dc and ac parts) and can be given as below [6]:

$$G = G_{dc} + G_{ac} \quad (9)$$

The G_{ac} is described well by Jonscher's power law relation [6]:

$$G_{ac} = A\omega^s \quad (10)$$

where A is a constant, ω is angular frequency ($\omega = 2\pi f$) and s is the dimensionless frequency exponent constant and gives us about the type of conduction mechanism knowledge in the studied compound. The exponent s is strongly depends on the temperature and mostly utilized to study possible conduction mechanism in material. In present study, the exponent s values were calculated from the conductivity measurement results with equation (10) and obtained results are given in Figure 5. The temperature dependent of the exponent s explained by some models in the literature. The first one is quantum mechanical tunneling (QMT) and according this model, s is not temperature dependent and remain constant [25]. The second one is overlapping large polaron tunneling (OLPT) model and according to this model, the exponent s decreases with temperature until a minimum value then it increases with increasing temperature [26]. The third one is small polaron model and according to this model, s value increases with increasing the temperature [27]. The last model or the fourth one is the correlated barrier hopping (CBH) model and this model proposes that the value of s decreases as the temperature increases [28].

It is realized that the *ac* region has two different linear slopes and these slopes denoted as s1 and s2 (see inset figures in Figure 5 (a)). The s1 is at the high frequency region whereas s2 is at the relatively middle or low frequency region. Figure 5 (b) depicts the temperature dependent exponent s behavior of LCO compound. The s1 first decreases with elevating temperature and reach a minimum value then increases with escalating temperature. Hence, in the s1 region the overlapping large polaron tunneling (OLPT) model

conduction mechanism is dominant mechanism. The $s2$ first remains constant then decreases with increasing temperature which shows us that the conduction mechanism includes both quantum mechanical tunneling (QMT) and correlated barrier hopping (CBH) model.

III.CONCLUSION

LaCrO$_3$ (LCO) compound has been synthesized using the solid-state reaction method. Structural and chemical analysis of LCO were carried out using SEM, EDX and XRD analyses. The crystal structures of the obtained LCO was investigated via XRD measurements and the measurement result revealed that the LCO has an orthorhombic crystalline structure. The calculated temperature dependent power law exponent, s is less than 1 for LCO compound for all temperatures as expected, the exponent s showed that the OLPT at high frequency region, the QMT and CBH conduction mechanisms observed at low frequency region for LCO depend on s exponent behavior, respectively. The calculated activation energies from admittance and dc conductance measurements are in close agreement with the each other.

ACKNOWLEDGEMENTS

REFERENCES

[1] Panpan, Z., Hongwei, Q., Heng, Z., Wei, L., Jifan, H. (2017). CO_2 gas sensors based on $Yb_{1-x}Ca_xFeO_3$ nanocrystalline powders. *Journal of Rare Earths*, 35(6), 602.

[2] Hilpert, K., Steinbrech, R.W., Boroomand, F., Wessel, E., Meschke, F., Zuev, A., Teller, O., Nickel, H., Singheiser, L., (2003). Defect formation and mechanical stability of perovskites based on LaCrO$_3$ for solid oxide fuel cells (SOFC). *J. Eur. Ceram. Soc.* 23, 3009-3020.

[3] Wang, S., Dong, Y., Lin, B., Gao, J., Liu, X., Meng, G., (2009). Fabrication of dense LaCrO$_3$ – based interconnect thin membrane on anode substrates by co-firing. *Mater. Res. Bull.,* 44, 2127-2133.

[4] Azad, A. M., Sudha, R., Sreedharan, O. M., (1990). Thermodynamic stability of LaCrO$_3$ by a CaF$_2$-based E.M.F. method. *J. Less Common Metals.* 166, 57–62.

[5] Rida, K., Benabbas, A., Bouremmad, F., Pen, M. A., Sastre, E., Martinez-Arias, A., (2008). Effect of strontium and cerium doping on the structural characteristics and catalytic activity for C_3H_6 combustion of perovskite LaCrO$_3$ prepared by sol-gel. *Appl. Catal. B Environ.,* 84, 457-467.

[6] Coskun, M., Polat, O., Coskun, F. M., Durmus, Z., Çaglar, M., Türüt, A., (2018). Frequency and temperature dependent electrical and dielectric properties of LaCrO$_3$ and Ir doped LaCrO$_3$ perovskite compounds. *Journal of Alloys and Compounds,* 740, 1012-1023.

[7] Adem, U., Mufti, N., Nugroho, A. A., Catalan, G., Noheda, B., Palstra, T. T. M., (2015). Dielectric relaxation in YMnO$_3$ single crystals. *Journal of Alloys and Compounds*, 638, 228–232.

[8] Chao, Z., Xiaofei, W., Zhaowu, W., Haitao, Y., Haisheng, L., Liben, L., (2016). Dielectric relaxation, electric modulus and ac conductivity of Mn-doped YFeO$_3$. *Ceramics International,* 42, 19461–19465.

[9] Jie, Z., Zhenxing, Y., Yu, L., Xiaohua, Z., Longtu, L., (2017). Understanding the thermally stimulated relaxation and defect behavior of Ti-containing microwave dielectrics: A case study of BaTi$_4$O$_9$. *Materials & Design,* 130, 479–487.

[10] Polat, O., Coskun, M., Coskun, F. M., Durmus, Z., Çaglar, M., Türüt, A. (2018). Os doped YMnO$_3$ multiferroic: A study investigating the electrical properties through tuning the doping level. *Journal of Alloys and Compounds,* 752, 274-288.

[11] Mori, M., Sammes, N. M., (2002). Sintering and thermal expansion characterization of Al-doped and Co-doped lanthanum strontium chromites synthesized by the Pechini method. *Solid State Ionics,* 146, 301–312.

[12] Vazquez, I. P. R., Angeles, J. C. R., Galicia, J. L. R., Jhu, K., Yanagisawa, K., (2004). Hydrothermal synthesis and sintering of lanthanum chromite powders doped with calcium. *Solid State Ionics,* 172, 389.

[13] Masato, I., Hirotsugu, T., Kyota, U., Tadashi, E., Masahiko, S. (1998). Microwave synthesis of LaCrO$_3$. *J. Mater. Chem.,* , 8, 2765–2768

[14] Zhang, G. J., Song, Y. W., Xiong, H., Zheng, J. Y., Jia, Y.Q., (2002). Synthesis and crystal structure of $La_{0.9}Ca_{0.1}Cr_{1-x}Ni_xO_3$ (x = 0.0–1.0) and electric conductivity of $La_{0.9}Ca_{0.1}Cr_{0.5}Ni_{0.5}O_3$. *Mater. Chem. Phys.,* 73, 101.

[15] Correa, H. P. S., Paiva-Santos, C. O., Setz, L. F., Martinez, L. G., Mello-Castanhe, S. R. H., Orlando M. T. D., (2008). Crystal structure refinement of Co-doped lanthanum chromites. *Powder Diff. Suppl.,* 23, S18.

[16] Li, D.-H., He, S.-F., Chen, J., Jiang, C.-Y., Yang, C., (2017). Solid-state Chemical Reaction Synthesis and Characterization of Lanthanum Tartrate Nanocrystallites Under Ultrasonication Spectra, *IOP Conf. Series: Materials Science and Engineering,* 242, 012023.

[17] Polat, O., Durmus, Z., Coskun, F. M., Coskun, M., Turut, A., (2018). Engineering the band gap of LaCrO$_3$ doping with transition metals (Co, Pd, and Ir), *J. Mater. Sci.,* 53, 3544–3556.

[18] Pudmich, G., Boukamp, B.A., Gonzalez-Cuenca, M., Jungen, W., Zipprich, W., Tietz, F. (2000). Chromite/titanate based perovskites for application as anodes in solid oxide fuel cells. *Solid State Ion.,* 135, 433–438.

[19] Fergus, J.W. (2004). Lanthanum Chromite-based Materials for Solid Oxide Fuel Cell Interconnects. *Solid State Ion.,* 171, 1–15.

[20] Kenji, Y., Naoshi, I., Yutaka, S., Yoshinobu, I., (2017). Absence of a polar phase in perovskite chromite $RCrO_3$ (R=La and Pr), *Materials Chemistry and Physics,* 190, 96-101.

[21] Khetre, S. M., Chopade, A. U., Khilare, C. J., Jadhav, H. V., Jagadale, P. N., Bamane,S. R., (2013). Electrical and dielectric properties of nanocrystalline $LaCrO_3$, *J. Mater. Sci: Mater. Electron.,* 24, 4361–4366.

[22] Nithya, V.D., Immanuel, J. R., Senthilkumar, S.T., Sanjeeviraja, C., Perelshtein, I., Zitoun, D., Selvan K. R., (2012). Studies on the structural, electrical and magnetic properties of $LaCrO_3$, $LaCr_{0.5}Cu_{0.5}O_3$ and $LaCr_{0.5}Fe_{0.5}O_3$ by sol–gel method, *Materials Research Bulletin,* 47 1861–1868

[23] Yong, S. L., Jae-Hoon, P., Jong, S. C., (2003). Frequency-Dependent Electrical Properties of Organic Light-Emitting Diodes. *Journal of the Korean Physical Society,* 42, 294-297.

[24] Coskun, M., Polat, O., Coskun, F. M., Durmus, Z., Çaglar, M., Türüt, A. (2018). The electrical modulus and other dielectric properties by the impedance spectroscopy of $LaCrO_3$ and $LaCr_{0.90}Ir_{0.10}O_3$ perovskites. *RSC Adv.,* 8, 4634–4648.

[25] Jung, W. H. (2008). AC conduction mechanisms of $Gd_{1/3}Sr_{2/3}FeO_3$ ceramic. *Physica B,* 403, 636-638.

[26] Wang, K., Chen, H., Shen, W.Z., (2003). AC electrical properties of nanocrystalline silicon thin films. *Physica B,* 336, 369-378.

[27] Abdelmoneim, H. M. (2010). Dielectric and ac conductivity of potassium perchlorate, KCLO{4}. *Acta Phisica Polonica A,* 117, 936-940.

[28] Elliott, S. R. (1977). A theory of a.c. conduction in chalcogenide glasses. *Philos. Mag. B.,* 36, 1291-1304.